



Patagonian and southern South Atlantic view of Holocene climate



M.R. Kaplan ^{a,*}, J.M. Schaefer ^{a,b}, J.A. Strelin ^{c,d}, G.H. Denton ^e, R.F. Anderson ^{a,b}, M.J. Vandergoes ^f, R.C. Finkel ^g, R. Schwartz ^a, S.G. Travis ^h, J.L. Garcia ^{e,i}, M.A. Martini ^d, S.H.H. Nielsen ^j

^a *Geochemistry, Lamont-Doherty Earth Observatory, Palisades, NY 10964, USA*

^b *Department of Earth and Environmental Sciences, Columbia University, New York, NY 10027, USA*

^c *Instituto Antártico Argentino (IAA), Argentina*

^d *Centro de Investigaciones en Ciencias de la Tierra (CONICET-UNC), Córdoba, Argentina*

^e *School of Earth and Climate Sciences and Climate Change Institute, University of Maine, Orono, ME 04469, USA*

^f *GNS Science, Lower Hutt 5010, New Zealand*

^g *Dept. of Earth and Planetary Sciences, University of California, Berkeley, CA 95064, USA*

^h *GCI, Soldiers Grove, WI 54655, USA*

ⁱ *Instituto de Geografía, Facultad de Historia, Geografía y Ciencia Política, Pontificia Universidad Católica de Chile, Chile*

^j *Kenex Ltd, New Zealand*

ARTICLE INFO

Article history:

Received 6 August 2015

Received in revised form

10 March 2016

Accepted 11 March 2016

Available online 23 April 2016

Keywords:

Cosmogenic dating

Patagonia

South Atlantic Ocean

Paleoclimate

Holocene

ABSTRACT

We present a comprehensive ^{10}Be chronology for Holocene moraines in the Lago Argentino basin, on the east side of the South Patagonian Icefield. We focus on three different areas, where prior studies show ample glacier moraine records exist because they were formed by outlet glaciers sensitive to climate change. The ^{10}Be dated records are from the Lago Pearson, Herminita Península-Brazo Upsala, and Lago Frías areas, which span a distance of almost 100 km adjacent to the modern Icefield. New ^{10}Be ages show that expanded glaciers and moraine building events occurred at least at 6120 ± 390 (n = 13), 4450 ± 220 (n = 7), 1450 or 1410 ± 110 (n = 18), 360 ± 30 (n = 5), and 240 ± 20 (n = 8) years ago. Furthermore, other less well-dated glacier expansions of the Upsala Glacier occurred between ~ 1400 and ~ 1000 and ~ 2300 and ~ 2000 years ago. The most extensive glaciers occurred over the interval from ~ 6100 to ~ 4500 years ago, and their margins over the last ~ 600 years were well within and lower than those in the middle Holocene. The ^{10}Be ages agree with ^{14}C -limiting data for the glacier histories in this area.

We then link southern South American, adjacent South Atlantic, and other Southern Hemisphere records to elucidate broader regional patterns of climate and their possible causes. In the early Holocene, a far southward position of the westerly winds fostered warmth, small Patagonian glaciers, and reduced sea ice coverage over the South Atlantic. Although we infer a pronounced southward displacement of the westerlies during the early Holocene, these conditions did not occur throughout the southern mid-high latitudes, an important exception being over the southwest Pacific sector. Subsequently, a northward locus and/or expansion of the winds over the Patagonia-South Atlantic sector promoted the largest glaciers between ~ 6100 and ~ 4500 years ago and greatest sea ice coverage. Over the last few millennia, the South Patagonian Icefield has experienced successive century-scale advances superimposed on a long-term net decrease in size. Our findings indicate that glaciers and sea ice in the Patagonian-South Atlantic sector of the Southern Hemisphere did not achieve their largest Holocene extents over the last millennium. We conclude that a pattern of more extensive Holocene ice prior to the last millennium is characteristic of the Southern Hemisphere middle latitudes, which differs from the glacier history traditionally thought for the Northern Hemisphere.

© 2016 Published by Elsevier Ltd.

1. Introduction

In pioneering work, [Mercer \(1968\)](#) inferred that during the Holocene glaciers in Patagonia may have been larger before the last millennium. He reasoned that, if correct, then such glacier behavior

* Corresponding author.

E-mail address: mkaplan@deo.columbia.edu (M.R. Kaplan).

must be related to climates far from Northern Hemisphere influences, where he assumed that Holocene maxima occurred during the European Little Ice Age. In Europe, over the last ~1000 years glaciers were at, or very close to, their maximum Holocene extents (e.g., [Grove, 2004](#); [Holzhauser et al., 2005](#); [Davis et al., 2009](#); [Schimmelpfennig et al., 2012](#)), and the conventional wisdom is that this period contained generally the most persistent cold conditions of the epoch ([Davis et al., 2009](#); [Kaufman et al., 2009](#)). However, it still remains unclear (e.g., [IPCC, 2014](#)) whether the Southern Hemisphere contains different expressions of Holocene glacier-climate from that in the Northern Hemisphere.

In Patagonia, as elsewhere, hypotheses such as Mercers' have been difficult to test robustly, because glacier deposits are difficult to date. ^{14}C dating is commonly used to construct Quaternary glacier chronologies. Although invaluable, this approach often only provides minimum-limiting, and less commonly maximum-limiting, ages for glacier landforms because they typically lack fossil matter. Moreover, when trying to resolve decadal-multidecadal glacier fluctuations over the last ~500 years, global ^{14}C variations may not permit assignment of unique ages, increasing the uncertainty of the dating approach (e.g., [Stuiver, 1978](#); [Porter, 1981](#)).

To this end, we obtained >80 ^{10}Be surface exposure ages that are used to reconstruct Holocene fluctuations of South Patagonian Icefield outlet glaciers ([Figs. 1 and 2](#)). We use recent advances in the ^{10}Be method ([Schaefer et al., 2009](#)) to date directly for the first time the exposure ages of moraine boulders and thus former glacier positions in Patagonia throughout the Holocene, including those that are <500 years old. We targeted the Lago Argentino area for study for several reasons. First, prior efforts documented which specific glaciers are particularly sensitive to climate and have left the most thorough landform and stratigraphic archives (e.g., [Mercer, 1968](#); [Strelin et al., 2014](#)). Earlier studies carried out detailed mapping, stratigraphic studies, and ^{14}C based reconstructions ([Mercer, 1968](#); [Aniya, 1995, 2013](#); [Aniya and Sato, 1995](#); [Aniya et al., 1997](#); [Malagnino and Strelin, 1992](#); [Strelin et al., 2011, 2014](#)). This study differs in approach from these valuable prior efforts, as we focus primarily on dating directly moraine boulders throughout the basin with ^{10}Be . In particular, we build on the recent work of [Strelin et al. \(2011, 2014\)](#), which demonstrated that in the Lago Argentino basin two independent dating approaches can indeed be used, ^{14}C and ^{10}Be , totaling the confidence and information obtained using both chronologies ([Figs. 2–5](#)). For

example, combining both approaches allows 1) information on times of glacier expansion (^{10}Be) and retraction (^{14}C); 2) replication of glacial-event ages within a given valley, including knowledge of the bounds of limiting ^{14}C ages; and 3) additional tests of the apparent similarities and differences between valleys.

We then use the record in Patagonia to ascertain broader patterns of paleoclimate in the middle latitudes, by linking the findings with records from the adjacent, downwind, South Atlantic Ocean. Core TN057-13 is near the southern position reached by the Antarctic Polar front and northern limit of sea ice ([Fig. 1](#)). This core thus affords records of sea ice, oceanographic, and climatic conditions also at higher latitudes than just at the drilling site ([Kanfoush et al., 2000](#); [Anderson et al., 2009](#); [Divine et al., 2010](#)). By ascertaining similarities between the terrestrial and marine realms, broader hemispheric patterns are reasonably inferred because it can be shown a regional climate change was not only experienced in southern Patagonia. Moreover, we compare our terrestrial-marine based findings with other records in the southern middle latitudes, including of the glacier history in New Zealand, to obtain a hemispheric-wide view.

2. Background and methods

Mountain glaciers respond sensitively to atmospheric change and they are well suited for past climate studies. In particular, glaciers in Patagonia respond directly to atmospheric conditions associated with the globally important Southern Hemisphere Westerly winds and Polar ocean-air climate systems ([Fig. 1](#)). 20th/21st century observations document that on timescales of several decades summer temperature dominates glacier history, with precipitation important locally and on the shorter-term ([Rignot et al., 2003](#); [Oerlemans, 2005](#); [Rivera and Casassa, 2004](#); [Naruse, 2006](#); [Carrasco et al., 2008](#); [Willis et al., 2012](#); [Casassa et al., 2014](#)). Also, Patagonian glaciers react rapidly to even small changes in climate given the temperate setting. This has led Patagonia to contain some of the fastest waning ice masses in the Southern Hemisphere at present ([Rignot et al., 2003](#); [Willis et al., 2012](#); [Casassa et al., 2014](#)).

2.1. Lago Argentino

The regional geology and climate of the Lago Argentino basin,

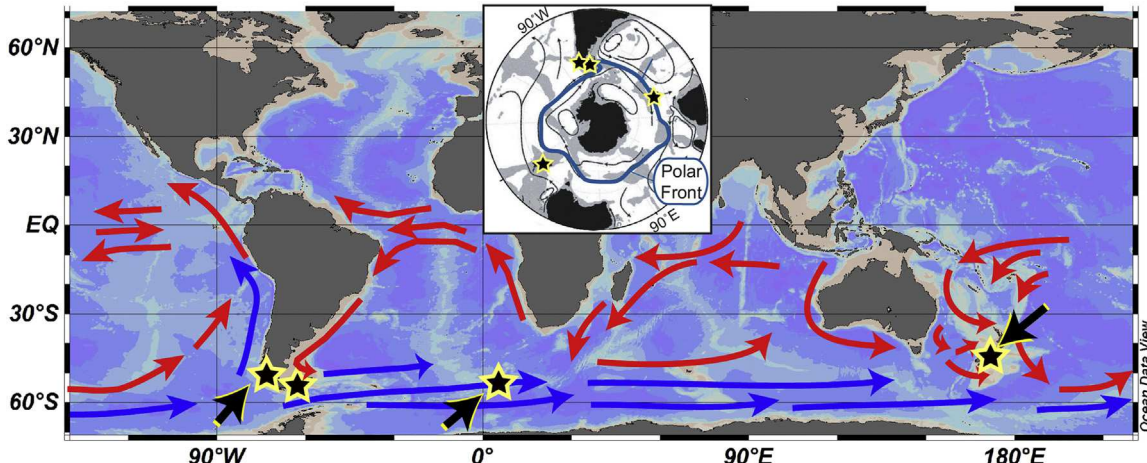


Fig. 1. Setting of places discussed in the text, in a Southern Ocean and Polar context. Sites discussed (stars) include, from left to right, southern Patagonia ([Figs. 2 and 3](#)), Isla de los Estados ([Fig. 7](#)), TN057-13 ([Figs. 6 and 7](#)) and South Island, New Zealand. For simplicity, currents are shown only for the Southern Hemisphere. Patagonia is downwind of the Southeast Pacific, where the cold Humboldt Current flows northward ([Fig. 2](#)). The location of TN057-13 is influenced by sub Antarctic climate regimes, being near the Polar front and northern limit of the sea ice influence (see text). Base image from Ocean Data View (ODV), <http://odv.awi.de/>.

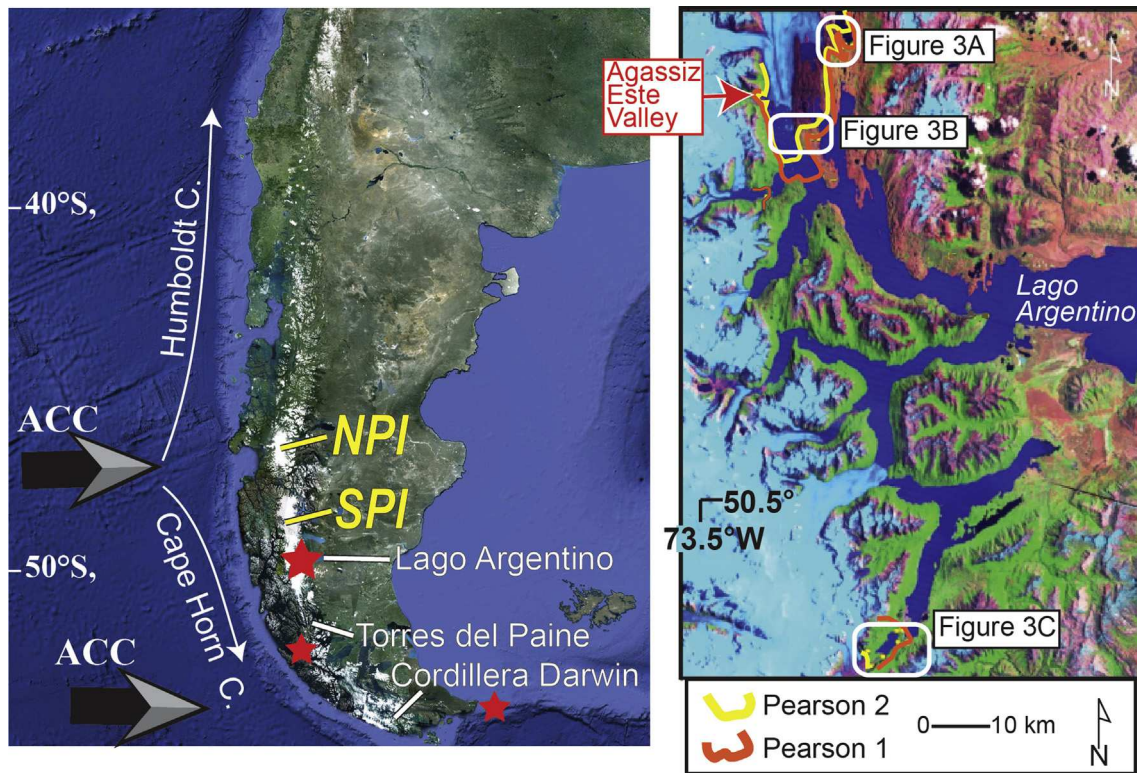


Fig. 2. Setting of the Lago Argentino basin. Pearson 1 and 2 are two prominent landform complexes found throughout the basin, with the former occurring up to several kilometers beyond the latter (Mercer, 1968; Aniya, 1995; Aniya and Sato, 1995; Aniya et al., 1997; Malagnino and Strelin, 1992; Strelin et al., 2014). Evidence for the extent of glaciers during the early Holocene is best preserved in Agassiz Este Valley, near the present ice front (Fig. 5; Strelin et al., 2014). Stars mark records shown on Fig. 7, including from the Lago Argentino area, the Chilean fjords, and Isla de los Estados.

south-central Patagonia, are summarized in detail in Strelin et al. (2011, 2014) and other works (e.g., Aniya, 1995). Two prominent landform complexes are found in the basin, which are informally named Pearson 1 and 2, with the former occurring up to several kilometers beyond the latter (Fig. 2) (Mercer, 1968; Strelin et al., 2014). Sequences of moraines of different ages are preserved at Lago Argentino, because subsequent ice front limits were less extensive and obliteration did not occur, and also, except in Agassiz Este, their sediments were not eroded by later outwash or river systems. Data from several sites allow us to reproduce key findings (Figs. 2 and 3) and see which dated landforms are preserved in respective valleys. For the glacier lobes we focus on in this study, moraines and subaerial outwash plains document that the ice margins were land-terminating or terrestrial based, except for a small section, which is the right (west) lateral margin of Upsala Glacier that presently faces Brazo Upsala (Fig. 2). Hence, calving processes are not an issue for our interpretations, given a focus on moraines associated with such subaerially formed features (e.g., also mapped fluvial channels, Fig. 3).

The ^{10}Be samples came from large boulders embedded in the crests of moraine ridges that appear stable. All boulders were photographed (e.g., Fig. 4) and their heights measured relative to the ground. For the most part, we sampled boulders at least 50 cm above the moraine matrix. We infer the ages on boulders rooted on the surfaces of moraine ridges likely represent the culmination of its construction, close to the end of a cold period and before onset of retreat due to warming. We sampled hard rhyo-dacitic and granitic boulders. Samples were taken from the upper 1–3 cm from the most stable flattish section of the boulder top, with a hammer and chisel or a drill. The azimuthal elevations of the surrounding landscape were measured using a compass and clinometer. We

used either a Trimble ProXH GPS system or a handheld Garmin, relative to the WGS 1984 datum, to measure position and altitude. Measurements were relative to benchmark datums near El Calafate established by the Argentine Military. Post processed uncertainties (1σ) were less than 50 cm for the Trimble system and <10 m (assumed) for the handheld; comparison of Trimble and handheld measurements at the same location typically agree within ~ 10 m. All samples were processed at the Cosmogenic Nuclide Laboratory at Lamont-Doherty Earth Observatory (Tables S1 and S2). We followed standard geochemical processing protocols explained in Schaefer et al. (2009) and Kaplan et al. (2011). Previously, Strelin et al. (2014) published 15 ^{10}Be ages as an outline of the glacier history.

Of crucial relevance for this paper, recent developments enable measurement of ^{10}Be concentrations of only 10^3 atoms/g for the first time in Patagonia. The method advances are summarized in Schaefer et al. (2009) and briefly, include: 1) ‘custom-made’ low process blanks made from deep mine beryl crystal, the details of which are provided in the Supplementary Material; and 2) recent developments at the Center of Accelerator Mass Spectrometry at Lawrence Livermore National Laboratory that make it possible to measure the low ^{10}Be concentrations. A custom-designed ion source produced high ^{9}Be ion currents ranging typically from 10 to 20 μA for the samples presented in Fig. 3.

Additional analyses are presented in the [Supplementary Material](#), where it is shown that different statistical central tendencies, i.e., mean, median, and associated errors, notably provide the same finding (Bevington and Robinson, 2003). The overall coherence of the datasets indicates that geological or geomorphic processes such as erosion or inheritance have minimal effects on these samples (i.e., within $1\text{--}2\sigma$ uncertainty), except for obvious

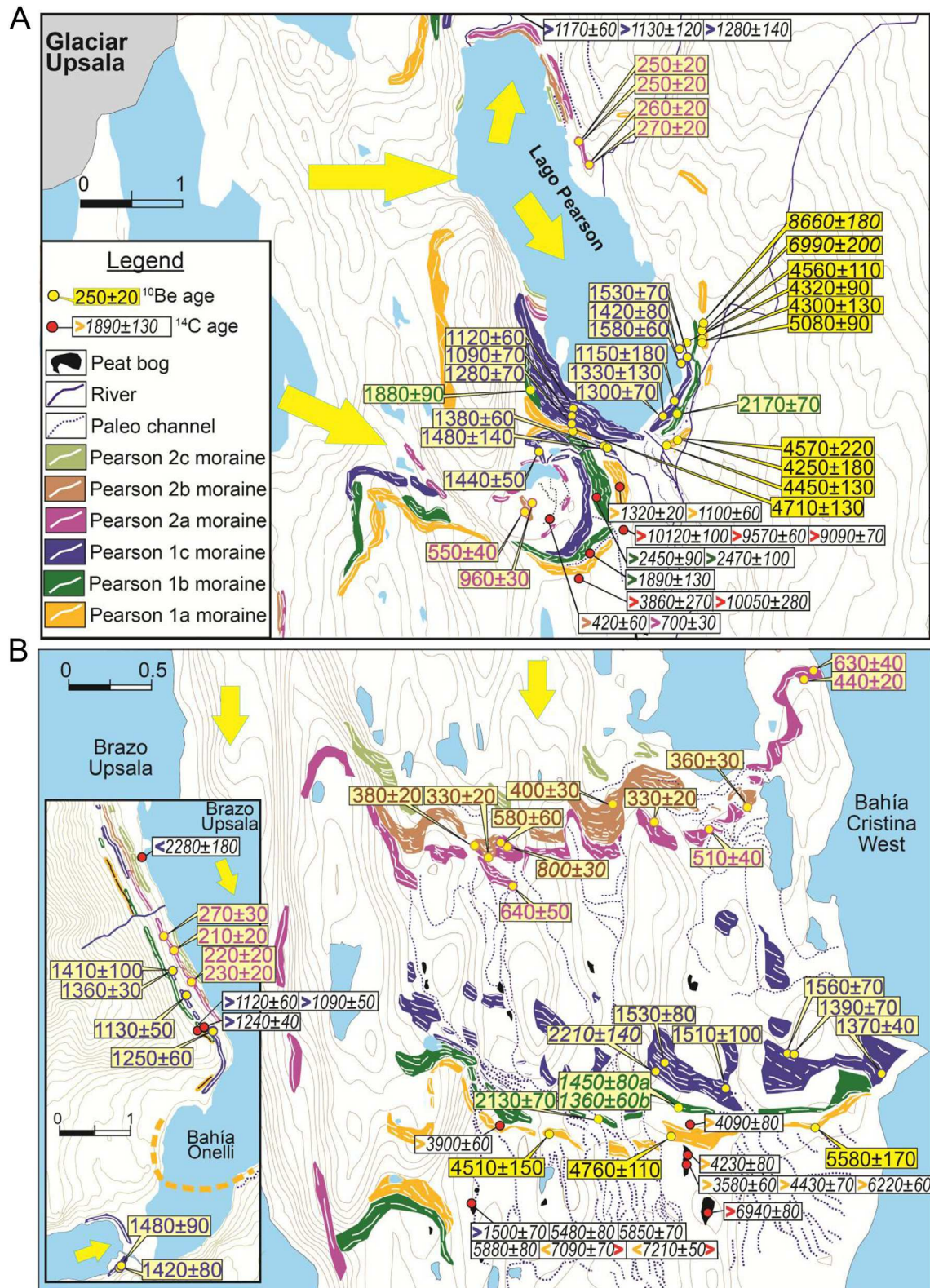


Fig. 3. A–C include geomorphic maps that show landforms that represent former glacier margins (from Strelin et al., 2014). Also shown are ^{10}Be ages ($\pm 1\sigma$ analytical uncertainty) (Figs. 4–6, Tables S1 and 2), and ^{14}C ages (Fig. 5; Table S3, from Strelin et al., 2014). The color of the symbol (< or >) in front of ^{14}C ages correspond to moraine ages shown on Fig. 5; if there is no symbol (Fig. 3B), then it is similar to the age of the event. For more explanation of the ^{14}C data, see Table S3. Known outliers are in italics. **A.** The Lago Pearson area. Note that there was no lake (i.e., no calving) around Lago Pearson when the outer moraines formed. **B.** The Herminita Peninsula, Brazo Upsala, and Bahía Onelli area. The legend is the same as in Fig. 3A. **C.** The Lago Frías valley. Note that the lakes did not exist (i.e., no calving), south of Brazo Sur, when the moraines formed.

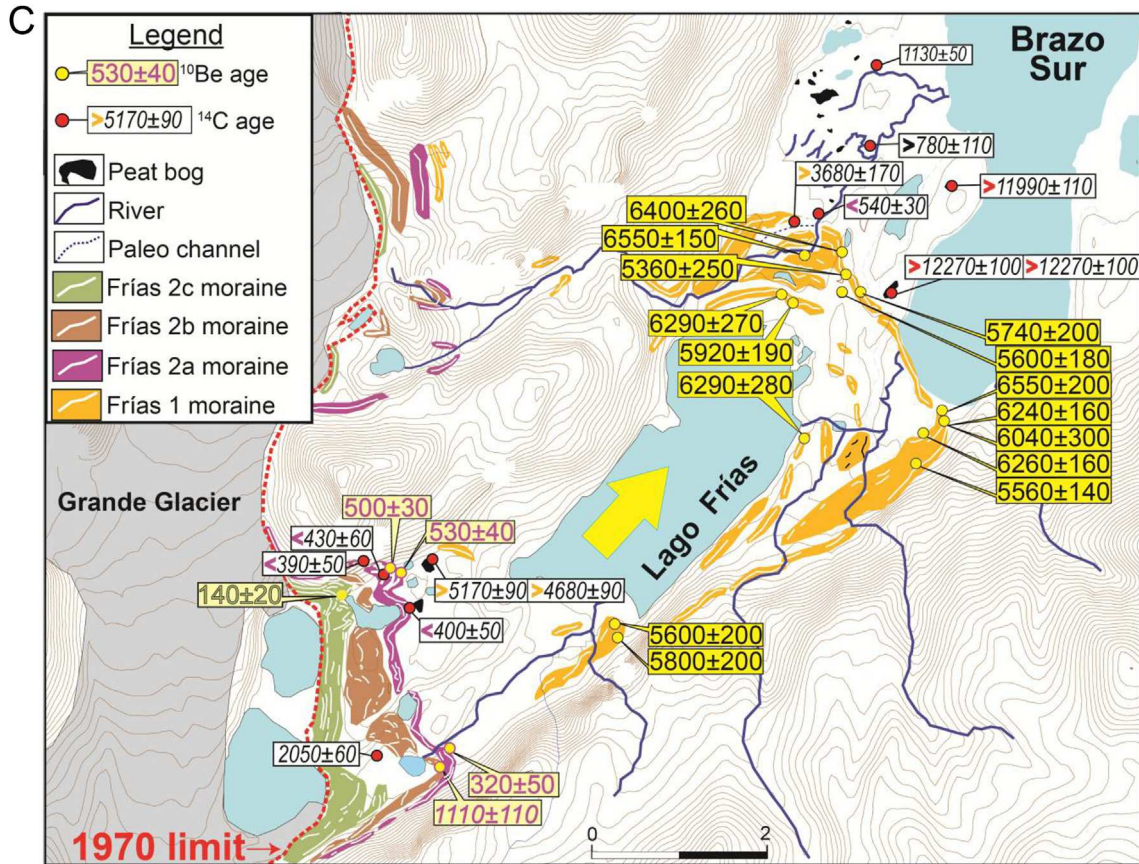


Fig. 3. (continued).

outliers. Given the relatively youth of the moraines, that is, less than ~6 ka for all samples, we assume erosion has had negligible effect, which is supported by our observations of boulder quality and characteristics (e.g., some boulders exhibit striations) in the field. For the arithmetic mean ages of the moraines discussed in the main text, we choose to present an error that includes propagation of those for the analytical AMS measurement and the production rate.

We minimize systematic uncertainties by using a recently-established, high-precision ^{10}Be production rate from the study area (Kaplan et al., 2011). This production rate is statistically indistinguishable from that in New Zealand, also in the middle latitudes of the Southern Hemisphere (Putnam et al., 2010). In Table S2, we provide ages according to the different currently accepted scaling schemes (Stone, 2000; Dunai, 2001; Desilets and Zreda, 2003; Pigati and Lifton, 2004; Lifton et al., 2008; Balco et al., 2008), although given a local calibration and low elevations and the latitude, ages between the various formulations agree within analytical uncertainties and thus do not alter our findings.

Last, all ^{10}Be ages are presented relative to the year of collection (e.g., FR-07-04 is 6190 years before 2007; Table S1). Whereas, all ^{14}C years are presented in years before present relative to 1950 (e.g., ka BP). In this paper, the difference (<60 years) does not change any findings when comparing chronometers, especially in the context of analytical uncertainties, but it is noted.

2.2. TN057-13 records

Details regarding collection, sampling, age models and other methods are summarized in Nielsen et al. (2007) and Anderson

et al. (2006, 2009, 2014). Evaluation of lithogenic and biogenic fluxes follow standard protocols as summarized in these references. Core TN057-13 is a 14-m-long jumbo piston core obtained in 1996 on cruise TN057 aboard the R/V Thomas Thompson. The core is located at 53°S, near the southern limit of the present-day polar frontal zone and 2° north of the average winter sea ice limit. Data in Fig. 6 are from Anderson et al. (2009), except for additional samples analyzed in this study throughout the Holocene. All data from core TN057-13 are archived at the National Climatic Data Center of the National Oceanic and Atmospheric Administration.

3. Results

3.1. Lago Argentino, southern South America

In the northernmost of the three areas (Fig. 2), near Lago Pearson, we dated moraines formed by two confluent lobes of the Upsala glacier flowing east and southeast (Fig. 3A). For both outlet lobes, moraines are steadily younger towards the present ice margin. Samples from the outermost moraine that wraps around the south end of Lago Pearson (Pearson 1a, yellow on Fig. 3A) have ^{10}Be ages of 5080 ± 90 to 4250 ± 180 years. In the area of the upper left lateral moraine, two boulders from short outermost moraine ridges yielded older ^{10}Be ages. The relation is unclear between these apparently older preserved crest slivers and the terminal~5–4 ka Pearson 1a moraine that wraps around Lago Pearson. Pearson 1b and c moraines returned ages from 2170 ± 70 to ~1 ka. Inside the latter, Pearson 1c limit, all moraines formed within the last ~1 ka. This includes unvegetated moraine ridges on the north end of Lago Pearson, where four of the youngest samples dated have ^{10}Be ages

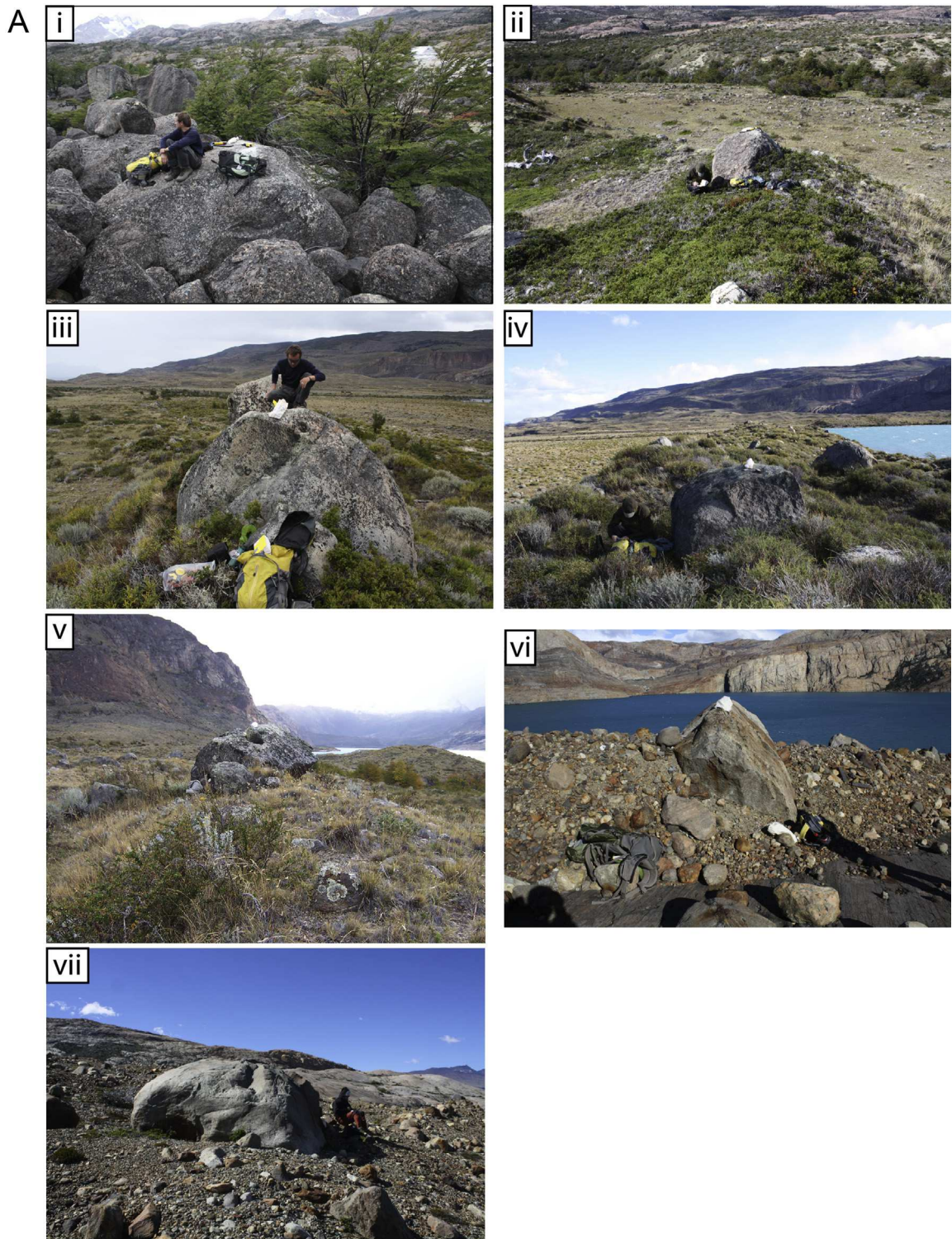


Fig. 4. A. Photographs of sampled boulders and moraines in the Lago Pearson area. i) Sample PE-10-02 (4300 ± 130) is on the top of a Pearson 1a left lateral crest. The photo is looking towards the northeast. Glacially-scoured terrain deglaciated in the early Holocene is seen beyond Pearson 1A. ii) PE-09-45 (4570 ± 220) is rooted in the top of a Pearson 1a left lateral crest. The photo is looking towards the northeast. iii) PE-10-04 (2170 ± 70) is rooted in the top of a Pearson 1b left lateral crest. The photo is looking towards the south-southwest. iv) PE-09-48 (1300 ± 70) is rooted in the top of a Pearson 1c left lateral crest. The photo is looking towards the southwest. In the background of the photo are outwash (subaerial) deposits from the Lago Pearson lobe that surround the lake. v) PE-07-32 (1120 ± 60) is rooted in the top of a Pearson 1c right lateral crest in front of Lago Pearson. The photo is looking northward. Lago Pearson is in the background. vi) PE-10-07 (270 ± 20) is rooted in a crest close to Lago Pearson. The photo is looking towards the west. In the background is the Fossil Canyon, which was the source of outlet lobe that formed this moraine. Note freshness of the deposit and it overlies striated bedrock. vii) PE-10-09 (250 ± 20) is in a crest close to Lago Pearson. The photo is looking towards the south. Note the freshness of the deposit given it is ~240 years old (Fig. 3A). **B.** Photographs of sampled boulders and moraines in the Hermitita Península-Brazo Upsala area. i) Sample PE-06-08 (1530 ± 80) on the top of the fifth Pearson 1c crest. The photo is looking towards the southeast and other Pearson 1 ridges are seen in the background (from Strelin et al., 2014). ii) Sample PE-07-04 (230 ± 20) is rooted in the top of a Pearson 2a right lateral crest adjacent to Bahía Upsala. **C.** Photographs of sampled boulders and moraines left by the former Frías Lobe, Fig. 3C. i) Sample FR-07-02 (6550 ± 200) is on the top of a Frías 1 crest. The photo is looking towards the north and Brazo Sur is seen in the background. ii) Sample FR-07-14 (6290 ± 270) is on the top of a Frías 1 crest. The photo is looking towards the northwest. Note the top of the boulder is well above surrounding vegetation. iii) Sample FR-07-31 (140 ± 20) is on the top of a Frías 2 crest. The whitish areas on top of the boulder are the sampled spots. The photo is looking towards the northeast and other Frías 2 ridges are seen in the background, including the area of samples FR-07-29 and -30.

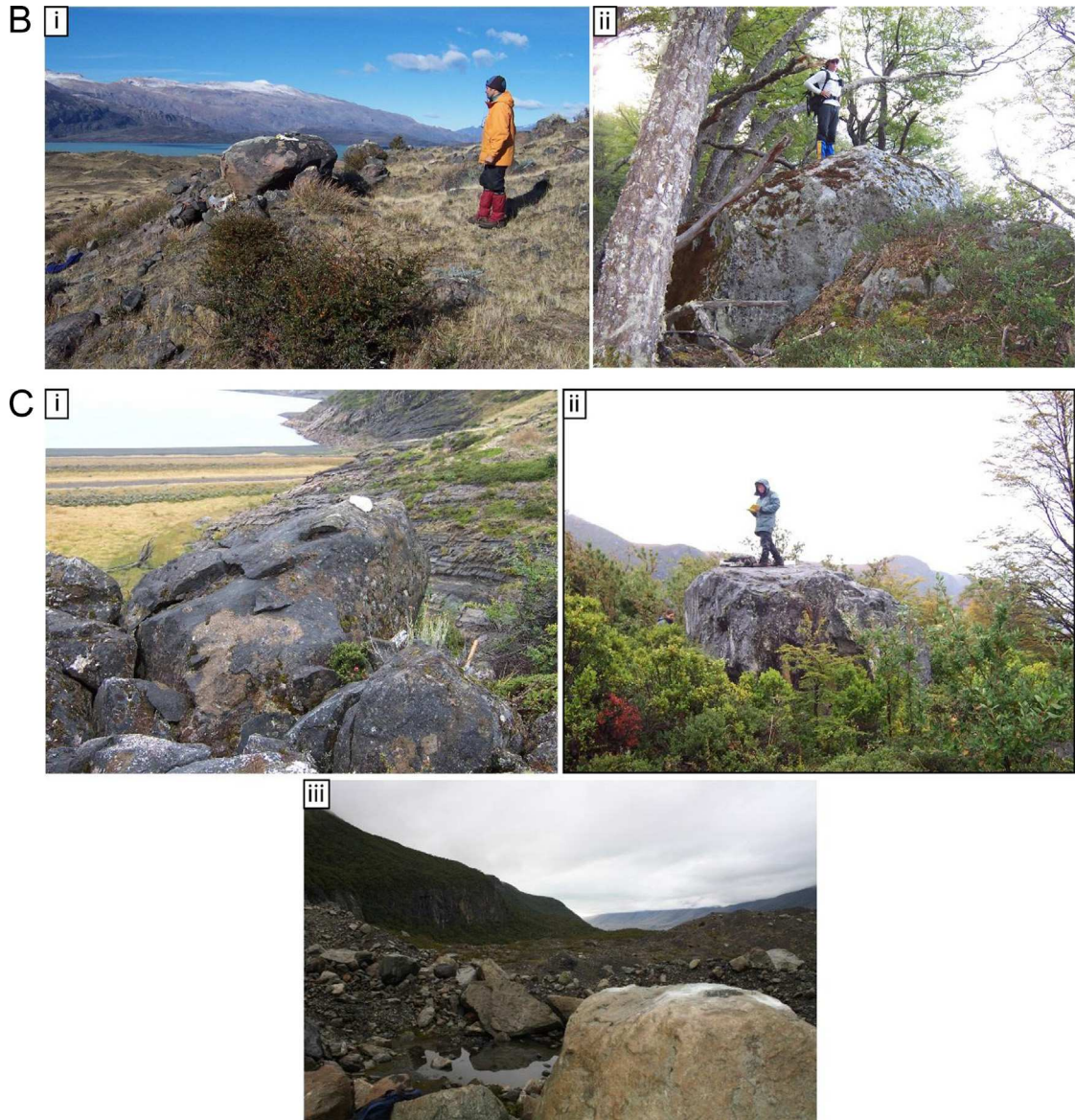


Fig. 4. (continued).

of between 250 ± 20 and 270 ± 20 years.

In the second area we focused on, around Herminita Península and Brazo Upsala, (Figs. 2 and 3B), moraines formed during southward expansions of the main Upsala Glacier lobe. Moraines are steadily younger towards the present ice margin. Specifically, three samples from the outermost moraine have ages of 5580 ± 170 , 4760 ± 110 , and 4510 ± 150 years. Inboard, Pearson 1b and c moraines returned ^{10}Be ages from 2130 ± 70 to 1360 ± 60 years (cf., Lago Pearson in Fig. 3A). And, inside the Pearson 1c limit, all moraines formed within the last ~ 700 years.

On the west side of Brazo Upsala we dated two right lateral moraines formed along the Upsala Glacier surface (inset on the left side of 3B). The upper Pearson 1c lateral moraine has ^{10}Be ages ($n = 4$) of 1410 ± 100 to 1130 ± 50 years. The lower Pearson 2a lateral moraine has ^{10}Be ages ($n = 4$) of 270 ± 30 to 210 ± 20 years. The lateral moraines document that the surface of the Upsala Glacier was at a lower elevation during the last few hundred years, after the higher Pearson 1c moraine formed (i.e., 1360 ± 30 to 1130 ± 50 years). In addition, a moraine located southwest of Bahía

Onelli, that formed after the Onelli and Upsala Glaciers separated, has two ^{10}Be ages of 1480 ± 90 and 1420 ± 80 years (from Strelin et al., 2014).

The third area where we focused ^{10}Be dating is around Lago Frías (Figs. 2 and 3C). Here, a prominent outermost moraine complex, locally mapped as Frías 1a, yielded 13 ages with a range from 6550 ± 200 (and 6550 ± 150) to 5360 ± 250 years. Inside this outer ~ 6 ka limit, a moraine near the south end of Lago Frías has ^{10}Be ages of 5800 ± 200 and 5600 ± 200 years; hence, the ^{10}Be ages on either side of Lago Frías are statistically indistinguishable. Closer to the present ice margin, boulders yielded ^{10}Be ages of 530 ± 40 to 140 ± 20 years. Only one outlier is identified (1110 ± 110) because it violates the relative stratigraphy and all other ages in the inner Frías valley.

For the Lago Argentino basin, for the sake of discussion, for the different outlet glaciers we provide average ages only for moraines that are the best dated; that is, with at least four statistically indistinguishable ^{10}Be ages on continuous traceable ridges (details in Supplementary Material). These mark expanded glaciers at

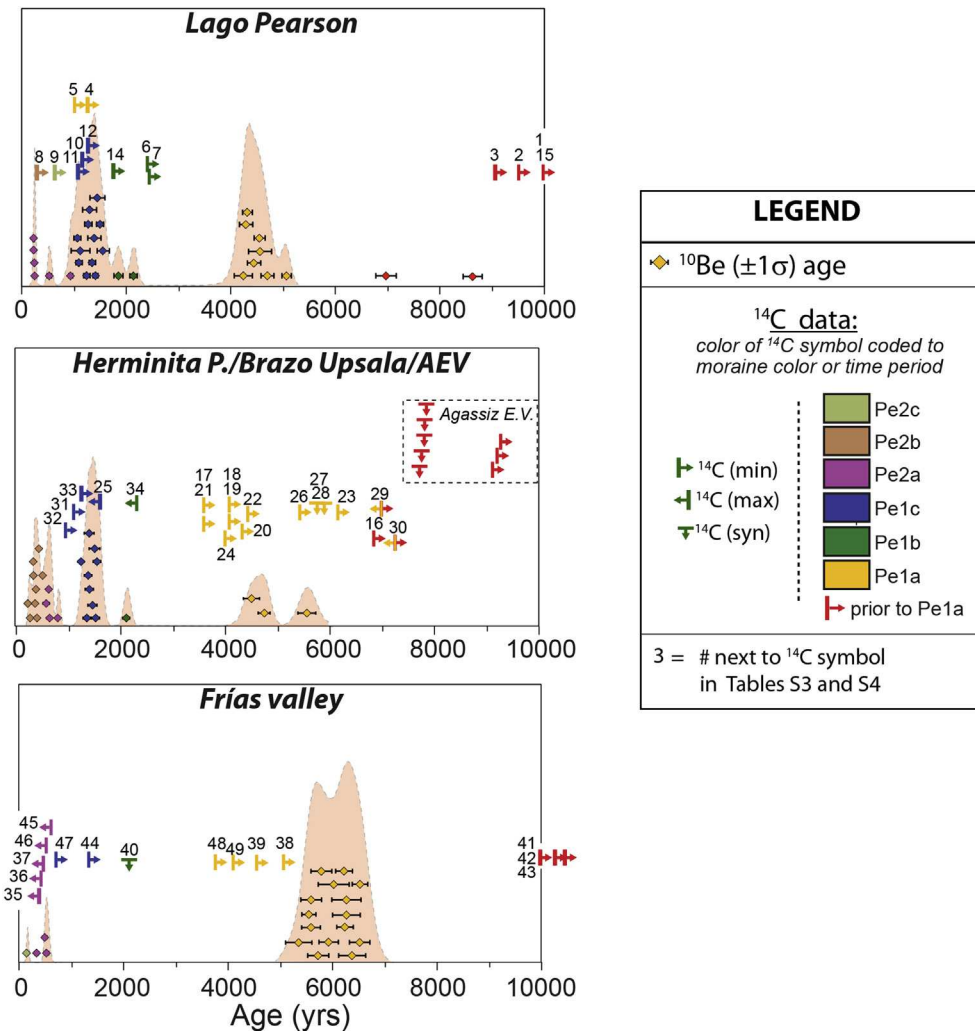


Fig. 5. Plot of ^{10}Be and ^{14}C ages used to define glacial histories in the Lago Argentino basin. All ^{10}Be and ^{14}C ages are listed in Tables S1–S4. The number next to each symbol corresponds to the ^{14}C ages (shown on Fig. 3) in Tables S3 and S4. Moraine names follow Fig. 3 and Strelin et al. (2014). Behind the ^{10}Be ages are summed probability distributions or 'camel humps' of all ages. On the Herminita Peninsula there are at least two Pearson 1a (Pe1a) moraines represented (Fig. 3B). Minimum-limiting ^{14}C ages older than 10 ka, which define the timing of deglaciation from Late Glacial limits (Strelin et al., 2011), are shown along the right border of the top and bottom panels. Ages from Agassiz Este Valley (AEV) are plotted in the middle panel; here, the ages >6 ka define glacial limits close to the present ice front (Strelin et al., 2014). This figure also highlights that ^{14}C ages often provide underestimated minimum- or overestimated maximum-limiting ages and thus only bracket the timing of moraine building events.

6120 ± 390 (Frías, $n = 13$, no outliers at $1-2\sigma$), 4450 ± 220 (at Lago Pearson, $n = 7$), $\sim 1450 \pm 90$ (Herminita Península-Onelli, $n = 8$), 1410 ± 110 (Lago Pearson, $n = 8$), 360 ± 30 years (on Herminita Península, $n = 5$, no outliers), 260 ± 10 years ago (Lago Pearson, $n = 4$), and 230 ± 20 (Herminita Península-Onelli, $n = 4$). Combining the four youngest ^{10}Be ages at both Lago Pearson (Fig. 3A) and west of Brazo Upsala (Fig. 3B) provides an age of 240 ± 20 years (no outliers), a limit that represents the last considerable dated advance of the Upsala Glacier (Fig. 2). Individual ^{10}Be ages on other less well-dated moraine ridges at Lago Argentino are consistent with the mean moraine ages provided above. For example, three different outermost moraine crests on the Herminita Península (Fig. 3B) also have three respective ages ranging from 5580 ± 170 to 4510 ± 150 years, consistent with Pearson 1a ages around the Lago Pearson and Frías areas (Fig. 3A and C). Interestingly, several of the outliers (e.g., 5080 ± 90 , Fig. 3A; 2210 ± 140 , Fig. 3B), although statistically older than the other ages on the crests they are from, are consistent overall with periods of expansion (Fig. 6). Perhaps, at least some of these outliers are on older

erratic boulders preserved in landforms that are younger for the most part.

3.2. TN057-13 and the southern South Atlantic

Most of the results were discussed in prior papers and here we only briefly review the salient observations, which include new data (Fig. 6) relevant for the Discussion in Section 4. In core TN057-13, the highest opal fluxes ($>6 \text{ g/cm}^2/\text{ka}$) are observed during the early Holocene, before ~ 6 ka, and subsequently values decrease towards $1 \text{ g/cm}^2/\text{ka}$ for the remainder of the epoch. Also during the early Holocene, lithogenic fluxes exhibit high viability, but this is superimposed on a net increase to almost $0.25 \text{ g/cm}^2/\text{ka}$ by ~ 7 ka. After ~ 3 ka, through the remainder of the Holocene, lithogenic fluxes to the South Atlantic generally decreased, although there are notable centennial-scale periods of increase (Fig. 6).

Sea ice fluctuations in the South Atlantic, including latitudinal changes, are discussed in Divine et al. (2010) and include data from TN057-13 (Fig. 6). Overall, there appears to be a positive correlation

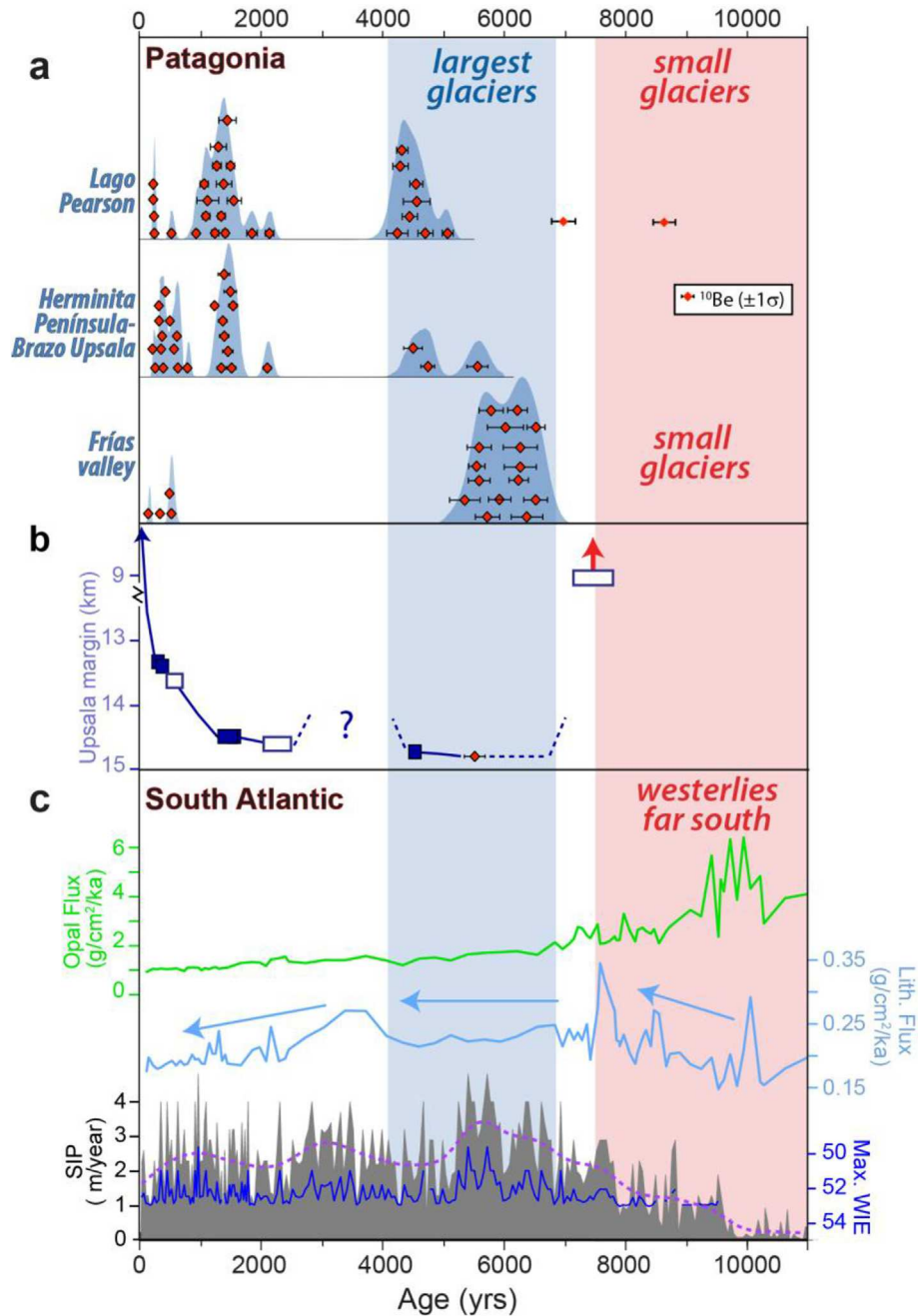


Fig. 6. Southern South American and South Atlantic climate patterns. a) ^{10}Be and summed probability density plots of all the ages shown in Fig. 3a–c. The ‘camel humps’ essentially reflect times of moraine formation. b) Time-distance plot for the Upsala ice front relative to modern, which incorporates data on Fig. 3A and B and average moraine ages. Closed and open rectangles symbolize ^{10}Be - and ^{14}C -dated frontal limits, respectively. Also shown is an advance ^{14}C -dated to ~8–7 ka in Agassiz Este Valley (Fig. 2; Strelin et al., 2014). Not shown is the 6.1 ± 0.4 ka advance of the Frías Glacier at the southernmost site (Fig. 3C). c) Opal and lithogenic flux data are from core TN057-13. Arrows in blue reflect overall net changes, as discussed in the text: WIE = winter ice edge latitude (dark blue); SIP = Sea ice presence (black); dashed purple line represents 1000-year smoothing. (For interpretation of the references to colour in this figure legend, the reader is referred to the web version of this article.)

between sea ice and lithogenic fluxes; and both of these proxies are negatively correlated with opal flux (at least) in the early Holocene. That is, the lowest sea ice values (e.g., months/yr) are in the earliest Holocene, before about 9 ka, when the winter ice edge appears to be consistently south of ~54°S. Towards the middle of the Holocene, although variable, there is a general net increase in months/yr of sea ice. Over the last several thousand years, the amount of sea ice fluctuates between ~1 and 4 months/yr along with maximum winter ice edge latitude. Our findings of a marked change from the

early to mid-Holocene, and then relatively sustained values after, are in agreement with earlier, lower resolution results from TN057-13 in Hodell et al. (2001).

4. Discussion

4.1. Lago Argentino

Eighty three ^{10}Be ages allow us to build on the known

framework of the glacier history in the Lago Argentino area (Section 1). We highlight that there are no observed Holocene moraines ^{10}Be dated prior to about 6 ka, with a possible exception of two older ^{10}Be ages (8660 ± 180 and 6990 ± 200) on small ridges preserved along the uppermost left lateral at Lago Pearson (Fig. 3A). To decipher the glacier behavior during the earliest Holocene prior to ~6 ka, we turn instead to the complementary ^{14}C chronology (Fig. 5), presented in Strelin et al. (2011, 2014). Their ^{14}C results include maximum-limiting ages on reworked pieces of wood in sediments in stratigraphic sections in Agassiz Este Valley, and on samples from basal sections of bog cores around Lago Anita and Lago Frías (Figs. 3 and 5; Table S3; Strelin et al., 2011, 2014). These data indicate that after the Late Glacial advances the South Patagonian Icefield retreated to close to present ice margins (Fig. 3A, C; Strelin et al., 2011, 2014). Any early Holocene advances (e.g., ~8–7 ka, in Strelin et al., 2014) of the glacier margin were within the subsequent maximum expansions (Fig. 3).

For the rest of the Holocene, we point out the following glacier patterns. First, a robust finding—reproduced among all sites studied—is that at least three different outlet glaciers of the South Patagonian Icefield exhibit maximum expansions in the middle Holocene, between ~6 ka and ~4.5 ka (Figs. 2 and 3). Strelin et al. (2014) defined the middle Holocene expansion from ~6 to 5 ka. The ^{10}Be data can be used to infer that either this period persisted longer than previously appreciated, or the younger 4.5 ka event was a subsequent pulse. Second, at all sites glacier advances were smaller in size after ~4.5 ka, and smaller after their limit at ~600–500 years ago. Over the last 600 years, glaciers are far less extensive than their earlier counterparts (Fig. 3). Decreasing ice extents after the middle Holocene are best revealed around Lago Pearson and on the Herminita Península, which have the most comprehensive moraine records, and in the Frías valley (Fig. 3A,B and C). Lateral moraines around Lago Pearson and west of Brazo Upsala also document that the surface of the Upsala Glacier reached lower levels during successive expansions, including at 230 ± 20 years ago (Fig. 3A, B).

Overall, the ^{14}C and ^{10}Be data are in agreement, excluding two outliers that occur on moraines on the Herminita Península (1450 ± 80 a/1360 ± 60 b and 2210 ± 140 , Fig. 3B) and one in the lower part of the Frías river valley (1110 ± 110 , Fig. 3C). We point out that the two chronometers do not need to overlap to be consistent. The ^{14}C ages discussed in Strelin et al. (2011, 2014), as well as in earlier studies (e.g., Aniya, 1995, 2013) often only provide minimum- or maximum-limiting ages and thus bracket the timing of moraine building events.

In addition to the common patterns highlighted above, we note that there are some differences among the valleys in terms of dated moraines (Fig. 3). However, we emphasize though that the observed pattern of maximum expansions in the middle Holocene, and smaller successive margins after, are independent of the (secondary) differences among the valleys – these patterns are replicated along ~100 km of the eastern side of the Icefield (Fig. 3). Strelin et al. (2014) discussed in depth the differences in moraines preserved between valleys and their possible causes. They demonstrated that such differences can be explained largely by preservation and happen chance (e.g. an example is shown in Fig. S1d) and variability in hypsometry, which leads to dissimilar glacier sensitivities to a regional climate event and responses in glacier length. In essence, during a given climate change, where the change in equilibrium line altitude (ELA) occurs in relation to glacier hypsometry can determine the magnitude of response in glacier length (Figs. 15 and 16 in Strelin et al., 2014). Mercer (1968) originally discussed that the Upsala Glacier illustrates the key role hypsometry can play, as ELA changes there consistently occur over a low surface gradient, causing a relatively large area to be affected.

Hence, it is not surprising that the Upsala Glacier moraines are widely separated and well-preserved at Lago Argentino (Fig. 3B; Mercer, 1968; Strelin et al., 2014). The argument of Strelin et al. (2014) is also partly based on the observation that climate does not vary in a major way over the 100 km along this eastern sector of the Icefield (Fig. 2), and the focus here is on past non-calving glaciers (except for small sections).

4.2. Southern South America

Our findings on Patagonian glacier evolution derived from moraines are in agreement with observations from other diverse data sets in southern South America. Paleotemperatures have been estimated in nearby areas for the time periods in which maximum and minimum glacier extents are observed in the Lago Argentino basin. Specifically, before 6 ka, when outlet glaciers were relatively small (Mercer, 1976; Moreno et al., 2009; Strelin et al., 2011, 2014; Menounos et al., 2013), estimates for onshore and offshore temperatures are ~2–3 °C warmer than present (e.g., Heusser, 1974; Lamy et al., 2010). Additionally, paleoecologic data document that the early Holocene was the warmest and driest part of the epoch, prior to the 20th century (e.g., Moreno and Leon, 2003; Markgraf et al., 2007; Whitlock et al., 2007; Kilian and Lamy, 2012).

In the earliest and middle Holocene, evidence for centennial-scale advances also exists both to the north and south of the Lago Argentino area (Mercer, 1976; Douglass et al., 2005; Moreno et al., 2009; Aniya, 2013). Douglass et al. (2005) estimated a ~300 m lowering of the equilibrium line altitude (ELA) at 46°S, corresponding to temperatures ~2–3 °C cooler than present (a maximum value if it is wetter as well as colder). The finding of prior efforts, of pronounced middle-early Holocene glacier expansions, much earlier than the last millennium, is consistent with our findings.

In the late Holocene, tree-ring and modeling-based temperature reconstructions agree, with estimates about 1–2 °C colder than present between ~600 and ~200 years ago, with the lowest temperatures earlier in this interval (Villalba et al., 2005). Others have also noted that glaciers in the middle latitudes of South America advanced during the last ~600 years (e.g., Mercer, 1976; Aniya, 1995, 2013; Aniya and Sato, 1995; Kilian and Lamy, 2012; Strelin et al., 2008). However, ^{10}Be dating directly ice marginal limits over the last ~600 years, defined by moraines, reveals that these advances were less expansive than those during the mid Holocene.

4.3. South Atlantic – southern South America

At site TN057-13, opal flux is interpreted to represent a proxy for upwelling in the Southern Ocean, which can be forced by the prevailing westerlies (Anderson et al., 2009). Lithogenic material deposited at the core site is mainly volcanic in origin and transported from the South Sandwich Islands by sea ice (Nielsen et al., 2007). Such material may increase due to sea surface temperature decline and sea ice survival (Anderson et al., 2006, 2009, 2014; Nielsen et al., 2007; Kanfoush et al., 2000; Divine et al., 2010). Regardless of the specific factors regulating changes in the deposition of lithogenic material, its flux reflects sea ice cover, which along with opal flux, are a function of the position of the westerly wind belt. That is, the position of the westerlies and the winter ice extent are positively correlated (e.g., equatorward westerlies = equatorward ice edge). Hence, we equate less (or more) sea ice with a southward (northward) displacement of the winds. We assume southward/northward displacement of the winds (or intensity) may be also associated with contraction/expansion of the wind belt, although our data alone cannot address such dynamics (e.g., Lamy et al., 2010; Björck et al., 2012).

Given that the South Atlantic Ocean and adjacent southern Patagonia are at a similar latitude and affected by the core of the westerly wind belt (Fig. 1) (e.g., Villalba et al., 1997; Yuan and Martinson et al., 2000; Stammerjohn et al., 2008), linking the terrestrial record with marine-based findings can reveal paleoclimate outlines that are regionally coherent over a broad swath of the southern latitudes (Fig. 6). We first highlight that we are mainly pointing out broad patterns and we are not necessarily focusing on correlating short-term individual peaks or events (e.g., less than a century), given differences between proxy types and some spatiotemporal variability might be expected. During the early Holocene, peak opal fluxes (Anderson et al., 2009) imply a far southerly position of the westerlies, which explains a climatic optimum with warm and dry conditions over the southern Andes (e.g., Moreno and Leon, 2003; Whitlock et al., 2007; Kilian and Lamy, 2012), causing glaciers to be similar to or behind present

limits (Figs. 3 and 5; Strelin et al., 2014). Perhaps the early Holocene is an analog for a warmer future in Patagonia. During the early Holocene, before ~6 ka, lithogenic fluxes in TN057-13 exhibit high variability, but this is superimposed on a net increase (Fig. 6). Subsequently, the greatest sea ice coverage in the South Atlantic over the Holocene, as indicated by months/yr and lithogenic flux reconstructions (Fig. 6), was over the time interval of the most extensive outlet glaciers, from ~6 to ~4.5 ka. Both South American and South Atlantic data are consistent therefore with colder air over these latitudes (~50–55°S) during the middle Holocene, when supposedly the westerly winds are more equatorward compared with the early part of the epoch. Our conclusions are in agreement with those in an earlier study in the South Atlantic by Hodell et al. (2001). Paleoecologic data are consistent with this finding (e.g., Markgraf et al., 2007; Whitlock et al., 2007; Schäbitz et al., 2013). After the middle Holocene, over the last few thousand years, the

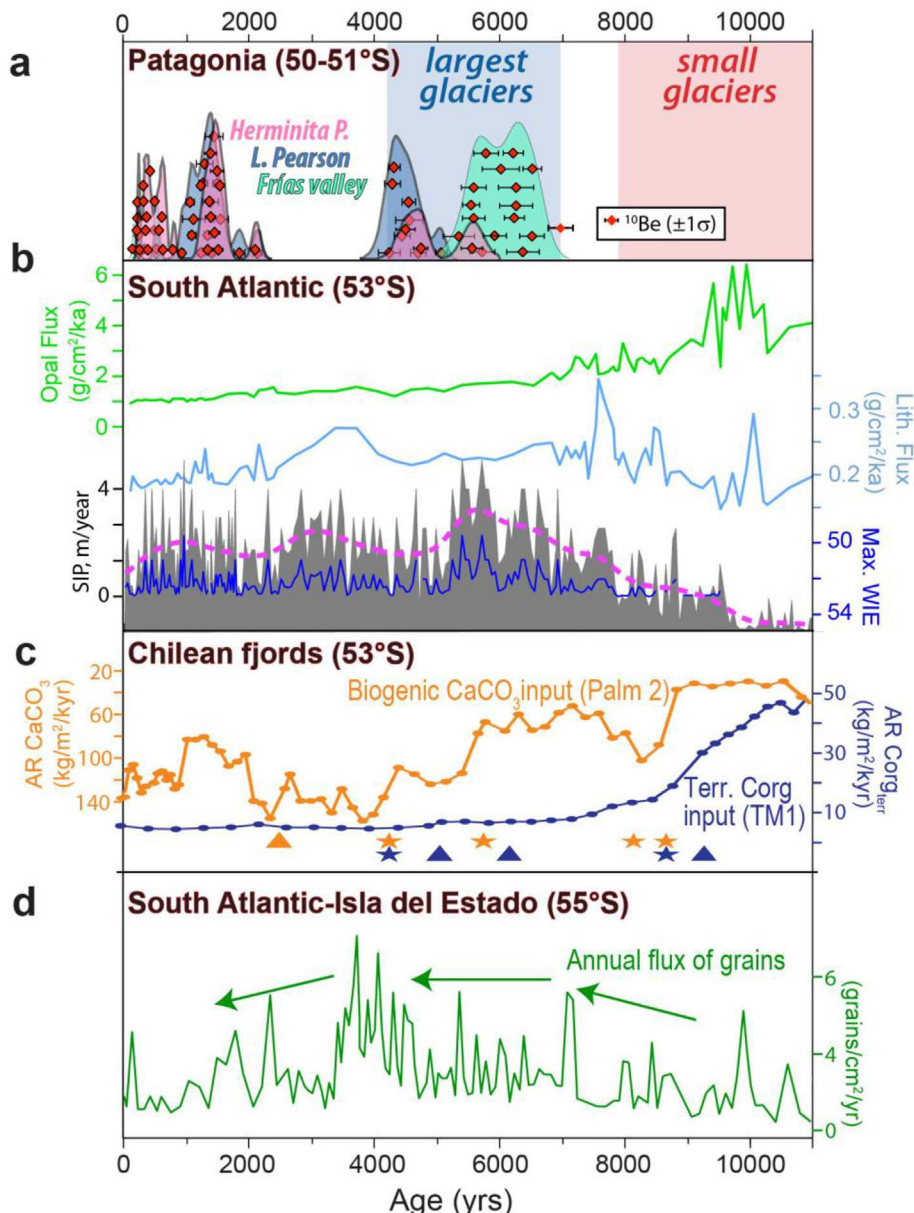


Fig. 7. Comparison of records from near southern South America and in the South Atlantic. a) and b) are from Fig. 6. c) Data are from Lamy et al. (2010). Biogenic CaCO₃ is inferred to be a proxy for salinity, which is a function of rainfall from the continent, with times of higher values reflecting the proximity of intense westerlies. Triangles indicate stratigraphic levels of ^{14}C ages and stars ash-layers. AR = accumulation rates; C_{org} = organic carbon. d) Data are from Björck et al. (2012). The annual flux of grains is inferred to be influenced by wind conditions.

findings from the South Atlantic and southern Patagonia indicate cold conditions generally remain sustained. There is a notable gap in dated moraines between ~4 and ~3 ka, which may imply glaciers were small at this time, or instead, any expansions were just inside the subsequent limit and not preserved. The data also may imply the westerlies do not exhibit their early Holocene southerly position in a persistent manner again (until the 20th century), and perhaps fluctuate between settings reached in the early and middle parts of the epoch.

For comparison to the findings shown on Fig. 6, we also mention other observations closer to southernmost South America (Fig. 7) and in the South Atlantic Ocean. We are not aware of high-resolution records for the entire Holocene from ocean sediments in the South Atlantic nearer to Patagonia (i.e., west of TN057), or in the Pacific away from the Chile shelf, within the latitude band of our records (~50–53°S) and the core of the westerlies. On the Pacific side of Patagonia, Lamy et al. (2010) studied a range of proxies for wind strength and precipitation in Chilean fjords and adjacent land bogs. On the South Atlantic side, as no high resolution records are available closer to southern Patagonia, instead, we present recent results from Björck et al. (2012), who inferred wind changes from deposition of locally-derived coarse grained lithogenic material on Isla de los Estados, ~55°S (building on prior studies, such as Ponce et al., 2011).

Before discussing comparisons between records, we first emphasize that we agree with the conclusion of Björck et al. (2012) that differences between records (especially distinct 'events') could be primarily due to what the proxies imitate and the seasons they represent. Also, the sensitivity of a proxy to changes in westerly strength could vary depending on where the core of the winds are located relative to the site (e.g., Fig. 7b, c). Nonetheless, for the sake of discussion, some broad patterns between records are highlighted. Notably, all records on Fig. 7 are consistent with the interpretation that the westerly winds are displaced far southward during the early Holocene. Lamy et al. (2010) inferred that perhaps (analogues) characteristics of the westerlies during the modern summer and winter typified the early and late Holocene, respectively. Subsequently, they shift back north by the middle Holocene. For the remainder of the Holocene, other paleoclimate records shown on Fig. 7 are consistent with our inference that the westerlies fluctuated between their early and middle Holocene positions. In addition, after recently synthesizing available data for the last ~30 ka from the South Atlantic Ocean, irrespective of the resolution, Xiao et al. (2016) also inferred southward displacement of the westerlies and early Holocene warmth, and subsequently, a generally more northward position for the rest of the epoch. Nonetheless, how the winds shift, that is, whether a displacement and/or contraction/expansion, remains an open question (Björck et al., 2012).

4.4. Other Southern Hemisphere comparisons

Briefly, we also compare past glacier behavior at the middle latitudes on both sides of the South Pacific Ocean – that is, the same type of proxy record that is largely responsive to summer conditions. Outside the sub Antarctic realm, New Zealand is the other major landmass in the middle latitudes of the Southern Hemisphere, besides South America, that contains glacier records for the last ~11,500 years (e.g., Grove, 2004; Kirkbride and Winkler, 2012; Schaefer et al., 2009; Solomina et al., 2015). As discussed in Sections 4.1–4.3, in the early Holocene glaciers are generally retracted in the warm dry Southern Andes (Moreno and Leon, 2003), with South Atlantic evidence in agreement and implying southward displacement (and perhaps contraction to higher southern latitudes) of the westerlies over this sector of the hemisphere (Fig. 6).

In contrast, in New Zealand the lowest ELAs and maximum glacier expansions are observed during the early Holocene (Putnam et al., 2012; Kaplan et al., 2013). Also, when southern Patagonian ice fronts are most extensive between ~6 and 4.5 ka, for comparison, glaciers in New Zealand are behind their earlier Holocene maxima (Gellatly et al., 1988; Schaefer et al., 2009; Putnam et al., 2012; Kaplan et al., 2013).

To explain the possible cause of early Holocene (as well as later in the Epoch) climate similarities and differences across the middle latitudes of the Southern hemisphere, we offer the following testable hypothesis. Over the last few decades, there have been opposing regional trends in mean climate states between the Antarctic Peninsula/southern Bellingshausen Sea and the western Ross Sea region, with contrasting temperatures, sea ice duration and concentrations (Yuan and Martinson, 2000; Stammerjohn et al., 2008). A strong Antarctic dipole reflects an out-of-phase relationship between the central/eastern Pacific and Atlantic sectors of the Antarctic (Pittock, 1980; Yuan and Martinson, 2000). Such patterns can be explained based on the eccentricity of the circulation or polar vortex around the South Pole (Fig. 8). We infer that sustained modes of relatively high eccentricity of the polar vortex during the early Holocene, similar to that of the last few decades (Fig. 8), typically favored a weak subtropical jet and a strong polar front jet in the Southern Hemisphere. In the early Holocene this caused warm winds and less sea ice around the South Atlantic-Weddell Sea sector (Section 4.3), but the opposite in the southwest Pacific sector including around New Zealand. Also, during this time New Zealand was likely affected by the relatively cool up-wind East Australian Current, linked to the behavior of the West Pacific Warm Pool and tropical climates (Fig. 1) (Putnam et al.,

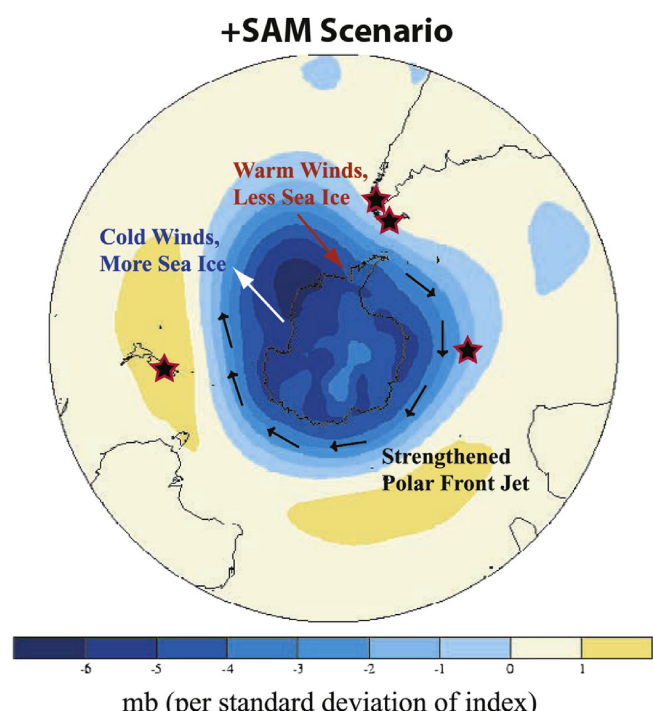


Fig. 8. From Stammerjohn et al. (2008). Schematic depiction of high-latitude polar ice-atmosphere responses to a positive Southern Annual Mode (SAM). In the case shown, the "eccentricity" of the polar vortex (Pittock, 1980) is a function of the response to a positive SAM, with the arrows schematically depicting wind anomalies during such a scenario. We hypothesize that such a scenario may have been typically dominant during the early Holocene. Other discussions of the dynamics of the polar vortex and its consequential spatiotemporal effects on Southern Hemisphere climate are in Villalba et al. (1997, 2005) and Pittock (1980).

2012). Moreover, given the higher latitudes of southern Patagonia, its climate may have been influenced by the far southward westerlies acting in concert with the duration of summer insolation, near the sea ice edge (Huybers and Denton, 2008). We speculate that, perhaps, a corollary is that the polar vortex and circulation around the South Pole was less eccentric (similar regional trends in mean climate states) during cold events of the last ~600 years, when glaciers on both sides of the Pacific Ocean appear to have advanced repeatedly (e.g., Gellatly et al., 1988; Kirkbride and Winkler, 2012; Schaefer et al., 2009; Putnam et al., 2012; Kaplan et al., 2013; Solomina et al., 2015).

We also point out another possible implication of a relatively eccentric polar and westerly circulation in the early Holocene. Prior to the Holocene, southward displacement of the westerly winds appears to occur with cold Northern Hemisphere stadials, such as during deglacial time, ~18 ka to 15 ka (Denton et al., 2010). The early Holocene may present a different scenario, whereby, parts of the mid to high southern latitudes instead experience southward displacement of the winds during Northern Hemisphere nonstadial or interglacial climates, in association with an eccentric polar and Westerly circulation. Future observations and modeling experiments can test such ideas, for example, on the effects of eccentricity of polar circulation and westerly winds in past climates.

5. Conclusions

Cosmogenic ^{10}Be dating directly on Holocene morainal landforms allows new insights into glacial histories in Patagonia, building on prior studies that have had to rely mainly on limiting ^{14}C ages. Furthermore, when the terrestrial South American record is linked with marine South Atlantic findings, this reveals paleoclimate patterns that were quasi-hemispheric. The Patagonian–South Atlantic view of the early Holocene is a time of general warmth, and dry conditions over the southern Andes, with retreated glaciers. Afterwards, glacial and marine-based records collectively are in agreement that colder conditions characterized the middle Holocene. A sustained northward displacement of the westerly wind belt (intensity and/or expansion) during the middle Holocene is compatible with the largest glacial expansions and sea ice concentrations. As in prior works, we observe advances during the last ~600 years (e.g., Mercer, 1976; Aniya, 1995, 2013; Aniya and Sato, 1995; Kilian and Lamy, 2012; Strelin et al., 2008, 2014). However, directly dating former glacier limits defined by landforms, based on the exposure duration of its constituent boulders, reveals that these advances were less expansive than during the middle Holocene.

From a broader perspective, there appear to be differences and similarities between paleoclimatic records across the middle latitudes of the Southern Hemisphere. On the one hand, glacier and marine based evidence suggest out-of-phase patterns between the Patagonia/South Atlantic and New Zealand/southwest Pacific sectors, during the earliest Holocene. Perhaps, these differences can be explained by invoking comparison with 20th/21st century opposing regional trends in mean climate states around the mid-high southern latitudes (e.g., Yuan and Martinson, 2000; Stammerjohn et al., 2008). Specifically, we hypothesize perpetual modes of relatively high eccentricity of the polar vortex, similar to that of the last few decades, favored warm winds and less sea ice around the South Atlantic–Weddell Sea, but the opposite in the southwest Pacific sector. On the other hand, a common finding is that during the Holocene glaciers on both sides of the South Pacific Basin were not the largest during the last millennium. Sea ice proxies from the South Atlantic Ocean are consistent with the glacier moraine based evidence. This raises the question of the degree to which glacier (or cyrospheric) histories in the Southern

Hemisphere are categorically analogues to defined patterns of Little Ice Age behavior in the Northern Hemisphere.

Acknowledgements

The research herein represents almost a decade of efforts by many individuals, which must be recognized. We are grateful to the Comer Science and Education Foundation, Instituto Antartico Argentino (IAA), Centro de Investigaciones en Ciencias de la Tierra (CICTERA), NOAA, NSF EAR-0902363 (which was funded through the American Recovery and Reinvestment Act of 2009, ARRA), and the Climate Center of LDEO and NASA GISS. Analysis of the Holocene portion of TN057-13 were supported by a grants/cooperative agreement from the National Oceanic and Atmospheric Administration. The views expressed herein are those of the authors and do not necessarily reflect the views of NOAA or any of its sub-agencies. Marcus Vandergoes was supported by the New Zealand Government through the GNS Global Change through Time Programme. Geol Cesar Torielli from Cordoba University (UNC) and numerous students from UNC who assisted us during the field work. For logistical support we thank Alejandro Tur and for discussion Aaron Putnam and Patricio Moreno. We thank Patricia Malone and Martin Fleisher for opal and thorium analyses, respectively, in TN057-13. Also, we are grateful to Hielo & Aventura (Jose Pera), Estancia Cristina (Daniel Moreno), Estancia La Querencia (Pedro Manger) and Administracion de Parques Nacionales (Guardaparque Fernando Spikermann). Last we thank Maarten Van Daele and an anonymous reviewer for helping us to improve substantially the manuscript. This is Lamont-Doherty Earth Observatory Contribution 7992.

Appendix A. Supplementary data

Supplementary data related to this article can be found at <http://dx.doi.org/10.1016/j.quascirev.2016.03.014>.

References

- Anderson, R.F., Fleisher, M.Q., Lao, Y., 2006. Glacial-interglacial variability in the delivery of dust to the central equatorial Pacific Ocean. *Earth Planet. Sci. Lett.* 242, 406–414.
- Anderson, R.F., Ali, S., Bradtmiller, L.I., Nielsen, S.H.H., Fleisher, M.Q., Anderson, B.E., Burckle, L.H., 2009. Wind-driven upwelling in the Southern Ocean and the deglacial rise in atmospheric CO₂. *Science* 323, 1443–1448.
- Anderson, R.F., Barker, S., Fleischer, M., Gersonde, R., Goldstein, S.L., Kuhn, G., Mortyn, P.G., Pahnke, K., Sachs, J.P., 2014. Biological response to millennial variability of dust and nutrient supply in the Subantarctic South Atlantic Ocean. *Philos. Trans. R. Soc. A Math. Phys. Eng. Sci.* 372, [10.1098/rsta.2013.0054](http://dx.doi.org/10.1098/rsta.2013.0054).
- Aniya, M., 1995. Holocene glacial chronology in Patagonia: Tyndall and Upsala glaciers. *Arct. Alp. Res.* 27, 311–322.
- Aniya, M., 2013. Holocene glaciations of Hielo Patagónico (Patagonia Icefield), South America: a brief review. *Geochem. J.* 47, 97–105.
- Aniya, M., Sato, H., 1995. Holocene glacial chronology of Upsala glacier at Peninsula Herminita, Southern Patagonia Icefield. *Glacier research in Patagonia. Bull. Glacier Res.* 13, 83–96.
- Aniya, M., Sato, H., Naruse, R., Skvarca, P., Casassa, G., 1997. Recent glacier variations in the Southern Patagonia Icefield, South America. *Arct. Alp. Res.* 29, 1–12.
- Balco, G., Stone, J.O., Lifton, N.A., Dunai, T.J.A., 2008. A complete and easily accessible means of calculating surface exposure ages or erosion rates from ^{10}Be and ^{26}Al measurements. *Quat. Geochronol.* 3, 174–195.
- Bevington, P., Robinson, D., 2003. *Data Reduction and Error Analysis for the Physical Sciences*. WCB McGraw-Hill, New York, p. 320.
- Björck, S., Rundgren, M., Ljung, K., Unkel, I., Wallin, Å., 2012. Multi-proxy analyses of a peat bog on Isla de los Estados, easternmost Tierra del Fuego: a unique record of the variable Southern Hemisphere Westerlies since the last deglaciation. *Quat. Sci. Rev.* 42, 1–14.
- Carrasco, J.F., Osorio, R., Casassa, G., 2008. Secular trend of the equilibrium-line altitude on the western side of the southern Andes, derived from radiosonde and surface observations. *J. Glaciol.* 54, 538–550.
- Casassa, G., Rodriguez, J., Loriaux, T., 2014. A New Glacier Inventory for the Southern Patagonia Icefield and Areal Changes 1986–2000. In: *Global Land Ice Measurements from Space*. Springer Praxis Books, pp. 639–660.
- Davis, P.T., Menounos, B.A., Osborn, G., 2009. Holocene and latest Pleistocene alpine

glacier fluctuations: a global perspective. *Quat. Sci. Rev.* 28, 2021–2033.

Denton, G.H., Anderson, R.F., Toggweiler, J.R., Edwards, R.L., Schaefer, J.M., Putnam, A.E., 2010. The last glacial termination. *Science* 328, 1652–1656.

Desilets, D., Zreda, M., 2003. Spatial and temporal distribution of secondary cosmic-ray neutron intensities and applications to in-situ cosmogenic dating. *Earth Planet. Sci. Lett.* 206, 21–42.

Divine, D.V., Koc, N., Isaksson, E., Nielsen, S., Crosta, X., Godtliebsen, F., 2010. Holocene Antarctic climate variability from ice and marine sediment cores: insights on ocean-atmosphere interaction. *Quat. Sci. Rev.* 29, 303–312.

Douglass, D.C., Singer, B.S., Kaplan, M.R., Ackert, R.P., Mickelson, D.M., Caffee, M.W., 2005. Evidence of early Holocene glacial advances in Southern South America from cosmogenic surface exposure dating. *Geology* 33, 237–240.

Dunai, T.J., 2001. Influence of secular variation of the magnetic field on production rates of in situ produced cosmogenic nuclides. *Earth Planet. Sci. Lett.* 193, 197–212.

Gellatly, A.F., Chinn, T.J.H., Rothlisberger, F., 1988. Holocene glacier variations in New Zealand: a review. *Quat. Sci. Rev.* 7, 227–242.

Grove, J.M., 2004. Little Ice Ages: Ancient and Modern. Routledge, London, New York, p. 718.

Heusser, C.J., 1974. Vegetation and climate of the southern Chilean Lake District during and since the last interglaciation. *Quat. Res.* 4, 290–315.

Hodell, D., Kanfoush, S., Shemesh, A., Crosta, X., Charles, C., Guilderson, T., 2001. Abrupt cooling of Antarctic surface waters and sea ice expansion in the south Atlantic sector of the southern ocean at 5000 cal yr B.P. *Quat. Res.* 56, 191–198.

Holzhauser, H., Magny, M., Zumbühl, H.J., 2005. Glacier and lake-level variations in west-central Europe over the last 3500 years. *Holocene* 15, 789–801.

Huybers, P., Denton, G.H., 2008. Antarctic temperature at orbital timescales controlled by local summer duration. *Nat. Geosci.* 1, 787–792.

IPCC, 2014. Climate Change 2013: the Physical Science Basis. Contribution of Working Group I to the Fifth Assessment Report of the Intergovernmental Panel on Climate Change, p. 1552.

Kanfoush, S.L., Hodell, D.A., Charles, C.D., Guilderson, T.P., Mortyn, P.G., Ninnemann, U.S., 2000. Millennial-scale instability of the Antarctic ice sheet during the last glaciation. *Science* 288, 1815–1818.

Kaplan, M.R., Strelin, J.A., Schaefer, J.M., Denton, G.H., Finkel, R.C., Schwartz, R., Putnam, A.E., Vandergoes, M.J., Goehring, B.M., Travis, S.G., 2011. In-situ cosmogenic ^{10}Be production rate at Lago Argentino, Patagonia: implications for late-glacial climate chronology. *Earth Planet. Sci. Lett.* 309, 21–32.

Kaplan, M.R., Schaefer, J.M., Denton, G.H., Doughty, A.M., Barrell, D.J.A., Chinn, T.J.H., Putnam, A.E., Andersen, B., Mackintosh, A.N., Finkel, R.C., Schwartz, R., Anderson, B.A., 2013. The anatomy of 'long-term' warming since 15 kyr ago in New Zealand based on net glacier snowline rise. *Geology* 41, 887–890.

Kaufman, D.S., Schneider, D.P., McKay, N.P., Ammann, C.M., Bradley, R., et al., 2009. Recent warming reverses long-term Arctic cooling. *Science* 325, 1236–1239.

Kilian, R., Lamy, F., 2012. A review of Glacial and Holocene paleoclimate records from southernmost Patagonia (49–55°S). *Quat. Sci. Rev.* 53, 1–23.

Kirkbride, M.P., Winkler, S., 2012. Timescales of climate variability, glacier response, and chronological resolution: issues for correlation of late Quaternary moraines. *Quat. Sci. Rev.* 46, 1–29.

Lamy, F., Kilian, R., Arz, H.W., Francois, J.-P., Kaiser, J., Prange, M., Steinke, T., 2010. Holocene changes in the position and intensity of the southern Westerly wind belt. *Nat. Geosci.* 3, 695–699.

Lifton, N., Smart, D., Shea, M., 2008. Scaling time-integrated in situ cosmogenic nuclide production rates using a continuous geomagnetic model. *Earth Planet. Sci. Lett.* 268, 190–201.

Malagnino, E., Strelin, J., 1992. Variations of Upsala glacier in southern Patagonia since the late Holocene to the present. In: Naruse, R., Aniya, M. (Eds.), Glaciological Researches in Patagonia, 1990. Japanese Society of Snow and Ice, pp. 61–85.

Markgraf, V., Whitlock, C., Haberle, S., 2007. Vegetation and fire history during the last 18,000 cal yr BP in Southern Patagonia: Mallín Pollux, Coyhaique, Province Aisén (45°41'30"S, 71°50'30"W, 840 m elevation). *Palaeogeogr. Palaeoclimatol. Palaeoecol.* 257, 492–507.

Menounos, B., Clague, J.J., Osborn, G., Davis, P.T., Ponce, F., Goehring, B.M., Maurer, M., Rabassa, J., Coronato, A., Marr, R., 2013. Latest Pleistocene and Holocene glacier fluctuations in southernmost Tierra del Fuego, Argentina. *Quat. Sci. Rev.* 77, 70–79.

Mercer, J., 1968. Variations of some Patagonian glaciers since the late glacial I. *Am. J. Sci.* 266, 91–109.

Mercer, J., 1976. Glacial history of southernmost South America. *Quat. Res.* 6, 125–166.

Moreno, P.I., Leon, A.L., 2003. Abrupt vegetation changes during the last glacial to Holocene transition in mid-latitude South America. *J. Quat. Sci.* 18, 787–800.

Moreno, P.I., Francois, J.P., Villa-Martinez, R.P., Moy, C.M., 2009. Millennial-scale variability in Southern Hemisphere westerly wind activity over the last 5000 years in SW Patagonia. *Quat. Sci. Rev.* 28, 25–38.

Naruse, R., 2006. The response of glaciers in South America to environmental change. In: Glacier Science and Environmental Change. Blackwell Publishing, Oxford, pp. 231–238.

Nielsen, S.H.H., Hodell, D.A., Kamenov, G., Guilderson, T., Perfitt, M.R., 2007. Origin and significance of ice-rafted detritus in the Atlantic sector of the Southern Ocean. *Geochem. Geophys. Geosyst.* 8, Q12005. <http://dx.doi.org/10.1029/2007GC001618>.

Oerlemans, J., 2005. Extracting a climate signal from 169 glacier records. *Science* 29, 675–677.

Pigati, J.S., Lifton, N.A., 2004. Geomagnetic effects on time-integrated cosmogenic nuclide production with emphasis on in situ ^{14}C and ^{10}Be . *Earth Planet. Sci. Lett.* 226, 193–205.

Pittock, A.B., 1980. Patterns of climatic variation in Argentina and Chile I. Precipitation, 1931–1960. *Mon. Weather Rev.* 108, 1347–1361.

Ponce, J.F., Borromei, A.M., Rabassa, J., Martinez, O., 2011. Late quaternary palaeoenvironmental change in western Staaten island (54.5°S, 64°W), Fuegian Archipelago. *Quat. Int.* 233, 89–100.

Porter, S.C., 1981. Glaciological evidence of Holocene climatic change. In: Wigley, T.M.L., Ingram, M.J., Farmer, G. (Eds.), Climate and History Studies on Past Climates and Their Impact on Man. Cambridge University press, Cambridge, pp. 82–110.

Putnam, A., Schaefer, J., Barrell, D.J.A., Vandergoes, M., Denton, G.H., Kaplan, M., Finkel, R.C., Schwartz, R., Goehring, B.M., Kelley, S., 2010. In situ cosmogenic ^{10}Be production rate calibration from the Southern Alps, New Zealand. *Quat. Geochronol.* <http://dx.doi.org/10.1016/j.quageo.2009.12.001>.

Putnam, A.E., Schaefer, J.M., Denton, G.H., Barrell, D.J.A., Finkel, R.C., Andersen, B.G., Schwartz, R., Chinn, T.J.H., Doughty, A.M., 2012. Regional climate control of glaciers in New Zealand and Europe during the pre-industrial Holocene. *Nat. Geosci.* 5, 627–630.

Rignot, E., Rivera, A., Casassa, G., 2003. Contribution of the Patagonia icefields of South America to sea level rise. *Science* 302, 434–436.

Rivera, A., Casassa, G., 2004. Ice elevation, areal, and frontal changes of glaciers from National Park Torres del Paine, Southern Patagonia Icefield Arctic. *Antarct. Alp. Res.* 36, 379–389.

Schäbitz, F., Wille, M., Francois, J.-P., Haberzettl, T., Quintana, F., Mayr, C., Lücke, A., Ohlendorf, C., Mancini, V., Paez, M.M., Prieto, A.R., Zolitschka, B., 2013. Reconstruction of paleoprecipitation based on pollen transfer functions – the record of the last 16 ka from Laguna Potrok Aike, southern Patagonia. *Quat. Sci. Rev.* 71, 175–190.

Schaefer, J.M., Denton, G.D., Kaplan, M.R., Putnam, A., Finkel, R.C., Barrell, D.J.A., Andersen, B.G., Schwartz, R., Mackintosh, A., Chinn, T., Schlüchter, C., 2009. High-frequency Holocene glacier fluctuations in New Zealand differ from the northern signature. *Science* 324, 622–625.

Schimelpfennig, I., Schaefer, J.M., Akçar, N., Ivy-Ochs, S., Finkel, R.C., Schlüchter, C., 2012. Holocene glacier culminations in the Western Alps and their hemispheric relevance. *Geology* 40, 891–894.

Solomina, O., Bradley, R.S., Hodgson, D.A., Ivy-Ochs, S., Jomelli, V., Mackintosh, A.N., Nesje, A., Owen, L.A., Wanner, H., Wiles, G.C., Young, N.E., 2015. Holocene glacier fluctuations. *Quat. Sci. Rev.* 111, 9–34.

Stammerjohn, S.E., Martinson, D.G., Smith, R.C., Yuan, X., Rind, D., 2008. Trends in Antarctic annual sea ice retreat and advance and their relation to El Niño–Southern Oscillation and Southern Annular Mode variability. *J. Geophys. Res.* 108.

Stone, J.O., 2000. Air pressure and cosmogenic isotope production. *J. Geophys. Res.* 105, 23753–23759.

Strelin, J., Casassa, G., Rosqvist, G., Holmlund, P., 2008. Holocene glaciations in the Ema glacier Valley, Monte Sarmiento Massif, Tierra Del Fuego. *Palaeogeography, Palaeoclimatology, Palaeoecology* 260, 299–314.

Strelin, J.A., Denton, G.H., Vandergoes, M.J., Ninnemann, U.S., Putnam, A.E., 2011. Radiocarbon chronology of the late-glacial Puerto Bandera moraines, Southern Patagonian Icefield, Argentina. *Quat. Sci. Rev.* 30, 2551–2569.

Strelin, J., Kaplan, M., Vandergoes, M., Denton, G., Schaefer, J., 2014. Holocene glacier chronology of the Lago Argentino Basin, Southern Patagonian Icefield. *Quat. Sci. Rev.* 101, 124–145.

Stuiver, M., 1978. Radiocarbon timescale tested against magnetic and other dating methods. *Nature* 273, 271–274.

Villalba, R., Cook, E.R., D'Arrigo, R.D., Jacoby, G.C., Jones, P.D., Salinger, M.J., Palmer, J., 1997. Sea-level pressure variability around Antarctica since A.D. 1750 inferred from subantarctic tree-ring records. *Clim. Dyn.* 13, 375–390.

Villalba, R., Masiokas, M., Kitzberger, T., Boninsegna, J.A., 2005. Biogeographical consequences of recent climate changes in the southern Andes of Argentina. In: Global Change and Mountain Regions: an Overview of Current Knowledge. Series: Advances in Global Change Research, vol. 23, pp. 157–166.

Whitlock, C., Moreno, P.I., Bartlein, P., 2007. Climatic controls of Holocene fire patterns in southern South America. *Quat. Res.* 68, 28–36.

Willis, M.J., Melkonian, A.K., Pritchard, M.E., Rivera, A., 2012. Ice loss from the Southern Patagonian ice field, South America, between 2000 and 2012. *Geophys. Res. Lett.* 39, 10, 1029/2012GL053136.

W. Xiao, O. Esper, R. Gersonde, 2016. Last Glacial – Holocene Clim. Var. Atl. Sect. South. Ocean 135, 115–137.

Yuan, X., Martinson, D.G., 2000. Antarctic Sea ice extent variability and its global connectivity. *J. Clim.* 13, 1697–1717.